

Determining the influential depth for surface reflectance of sediment by BRDF measurements

H. Zhang and K. J. Voss

Physics Department, University of Miami, Coral Gables, FL 33124
hzhang@physics.miami.edu, voss@physics.miami.edu

R. P. Reid

Rosenstiel School of Marine and Atmospheric Science, University of Miami,
4600 Rickenbacker Cswy, Miami, Florida, 33149
preid@rsmas.miami.edu

Abstract: We measure the Bi-directional reflectance distribution function (BRDF) of ooid sand layers with three particle size distributions (0.5-1mm, 0.25-0.5mm and 0.125-0.25mm) and layer thicknesses on a reflecting mirror to determine the influential depth in the optical region at wavelengths of 658 nm (red), 570 nm (green) and 457 nm (blue). The hemispherical reflectance (albedo) was used as an indicator of BRDF changes between different layers. Measurements are carried out on both dry and water wetted grains. The results indicate that for both dry and wet and all size distributions, the influential depth is at most 2mm.

©2003 Optical Society of America

OCIS codes: (010.4450) Ocean optics; (280.0280) Remote sensing; (290.5850) Scattering, particles; (030.5620) Radiative transfer; (300.0300) Spectroscopy; (350.4990) Particles.

References and links

1. B Hapke, *Theory of reflectance and emittance spectroscopy* (Cambridge University Press, New York, 1993).
2. H. Zhang, K. J. Voss, R. P. Reid and E. Louchard, "Bi-directional reflectance measurements of sediments in the vicinity of Lee Stocking Island, Bahamas," *Limnol. Oceanogr.* **48**, 380 (2003).
3. K. J. Voss, A. L. Chapin, M. Monti and H. Zhang, "Instrument to measure the bidirectional reflectance distribution function of surfaces," *Appl. Opt.* **39**, 6197 (2000).
4. J.D. Milliman, *Recent Sedimentary Carbonates Part 1: Marine Carbonates* (Springer-Verlag Berlin, 1974).
5. K. J. Ranson, J. R. Irons and C. S. Daughtry, "Surface albedo from Bidirectional reflectance," *Remote Sens. Environ.* **35**, 201 (1991).
6. S. A. Twomey, C. F. Bohren and J. L. Mergenthaler, "Reflectance and albedo differences between wet and dry surfaces," *Appl. Opt.* **25**, 431 (1986).
7. M. Kuhl, C. Lassen C and B. Jorgensen, "Light penetration and light intensity in sandy marine sediments measured with irradiance and scalar irradiance fiber-optic microprobes," *Mar. Ecol. Prog. Ser.* **105**, 139 (1994).
8. M. Kuhl and B. Jorgensen, "The light field of microbenthic communities: radiance distribution and microscale optics of sandy coastal sediments," *Limnol. Oceanogr.* **39**, 1368 (1994).
9. S. Chandrasekhar, *Radiative transfer* (Dover Publications, New York 1981).
10. S. Liang, "An investigation of remotely-sensed soil depth in the optical region," *Int. J Remote Sens.* **18**, 3395 (1997).
11. K. Stammes, S. Tsay, W. Wiscombe and K. Jayaweera, "Numerically stable computer code for discrete-ordinate-method radiative transfer in multiple scattering and emitting layered media," *Appl. Opt.* **27**, 2502 (1988).
12. M. I. Mishchenko, "Light scattering by size-shape distributions of randomly orientated axially symmetric particles of a size comparable to a wavelength," *Appl. Opt.* **32**, 4652 (1993)

1. Introduction

The Bi-directional reflectance distribution function (BRDF) is defined as the ratio of the radiance scattered by a surface into a given direction to the collimated power incident on a

unit area of the surface [1]. The BRDF is the fundamental parameter needed to accurately predict how light is reflected from a surface. In both active and passive remote sensing, it is a critical parameter in determining the received signal. In addition, it is an important parameter for radiative transfer modeling of the light field in shallow water. Recently we have made BRDF measurements on various benthic sediments and found they can be very anisotropic[2]. Our ultimate goal is to develop a predictive model of the BRDF based on the physical characteristics of the sediment. When comparing the BRDF measurements to physical parameters of the sediment such as surface morphology, packing structure, and dissolved organic matter, it is important to know the sediment layer depth that influences the BRDF to properly characterize the sediment. To determine the depth which influences the BRDF, we have carried out laboratory BRDF measurements, embedding a reflective mirror at different depths in an ooid sand sediment. Measurements have been done on both dry and wet samples at 3 visible wavelengths. Albedos are then calculated from the BRDF in order to quantitatively determine the small variations of the reflectance factors.

2. Instrument, calibration and sample descriptions

Our in-situ BRDF-meter [3] uses fiber optics to collect light from 107 fixed viewing angles located from 5 to 65 degrees in zenith and from 5 to 345 degrees in azimuth and bring light to a cooled CCD array camera (Apogee AP 260). Three colors of LED's (red at 658 nm, green at 570 nm, and blue at 475 nm in wavelength) located from 0 to 65 degrees in zenith sequentially illuminate the sample area. The illuminated area ranges from a 1.5 cm-diameter circle at 0 degree incidence to a 3.8 cm by 1.5 cm ellipse at 65 degrees. Calibration is done by taking the ratio of the measured reflectance in a given direction to that which a 100% lambertian reflector would have, thus the data presented in this form is the bi-directional reflectance factor (REFF)[1].

On a stable machined surface, such as a Labsphere calibration plaque, the relative REFF difference between measurements is less than 0.1% which includes small alignment surface level variations. The integrated quantity, albedo, has typical relative variations of 0.03%, up to 0.3% in rare cases at larger illumination angles, thus the instrument is itself quite stable.

Ooid sands were collected in the vicinity of Cat Cay, Bahamas in 1999. The lamellar carbonate coatings of these ooid grains were formed in high-energy tidal channels and provided a highly reflective, lustrous surface for BRDF measurements [4]. The sediment was bleached with sodium hypochlorite (5.25%) for 24 hours and then sieved into three sizes, 0.5-1 mm (coarse sand, sample A), 0.25-0.5 mm (medium sand, sample B) and 0.125-0.25 mm (fine sand, sample C). The fine (C) and medium (B) sand-sized ooids are mainly spherical particles while the coarse sand (A) is a mixture of spherical ooid grains and broken shells. Although the measurements shown here are not *in situ* and the sample preparation processes has eliminated possible effects such as organic coatings and absorbing medium, the results may still allow us to determine the influential depth in a natural sediment. Once we can determine the influential thickness of such "ideal" grains then we can incorporate other factors such as previously mentioned to extend this work. However it is likely that, because of absorption, these other factors would decrease the influential depth to even less than we found.

Grain layers of thickness 6.8 mm (depth I), 4.5 mm (II), 2.9 mm (III), 2 mm (IV) and 1.2 mm (V) were formed for these three samples by first laying aluminum plates with various thickness combinations on the bottom of the sample holder, then placing either a mirror or a black tile on top (Fig. 1). Grains were slowly poured into the holder to form a thin layer

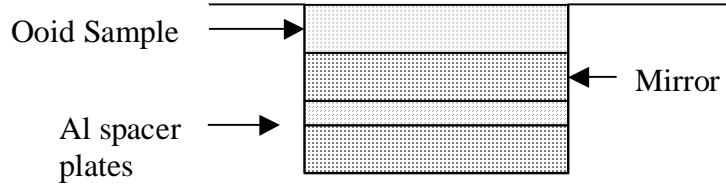


Fig. 1. Illustration of sample holder. Aluminum spacer plates are placed below the mirror or black plate to achieve the desired sample layer thickness.

with the desired thickness above the mirror or black tile. The plate containing the sample holder was tapped and shaken to settle down the grains. To level the surface, the edge of a plastic ruler was moved along different directions to make it macroscopically smooth and orientation independent. Four measurements were made for each surface to minimize the sample inhomogeneity, and between each measurement the sample holder plate was rotated 90 degrees to eliminate any remaining orientation biases of the sample surface. At each thickness, after a dry surface was measured, the BRDF of a wetted surface was also measured. Water was carefully dripped in from the edge of the sample holder until the grains were thoroughly saturated and a small amount of water ponded on the surface. Then a small piece of paper towel was touched to the surface to absorb the excess water. We were careful in this procedure to try to keep the sample surface morphology as close as possible to the corresponding dry surface. The ooids absorb little or no water, and measurements were performed on the wetted surface within 20 minutes of introducing the water. After the wet measurements were done, the sample surface was checked with the edge of a ruler to make sure the sample thickness remained constant during the measurements

3. Typical data

By definition [1], the BRDF may be expressed as:

$$BRDF(\theta_i, \phi_i; \theta_r, \phi_r) = \frac{J(\theta_i, \phi_i)r(\theta_i, \theta_r, g)}{J(\theta_i, \phi_i)\cos(\theta_i)} \equiv \frac{r(\theta_i, \theta_r, g)}{\cos(\theta_i)}$$

where $J(\theta_i, \phi_i)$ is the incident irradiance per unit area in the direction defined by a zenith angle θ_i and an azimuth angle ϕ_i , $J(\theta_i, \phi_i)r(\theta_i, \theta_r, g)$ is the reflected radiance in the direction (θ_r, θ_r, g) with phase angle g given by:

$$\cos g = \cos \theta_i \cos \theta_r + \sin \theta_i \sin \theta_r \cos(\phi_r - \phi_i)$$

and $r(\theta_i, \theta_r, g)$ is the bi-directional reflectance. As mentioned in Section 2, after the calibration process the reduced data is REFF given by:

$$REFF(\theta_i, \phi_i; \theta_r, \phi_r) = \frac{r(\theta_i, \theta_r, g)}{r_L} \equiv \frac{r(\theta_i, \theta_r, g)}{\cos(\theta_i)/\pi} = \pi BRDF(\theta_i, \phi_i; \theta_r, \phi_r)$$

where $r_L = \cos(\theta_i)/\pi$ is the bi-directional reflectance of a perfect Lambertian surface with 100% reflectance. One of the advantages of using REFF over bi-directional reflectance is that it is easily compared to a perfect Lambertian surface. Throughout this work, the incident azimuth ϕ_i is specified to be 0° thus the REFF is simplified to $REFF(\theta_i; \theta_r, \phi_r)$. The REFF are represented in both contour plots and plots against phase angles to manifest the angular variations. The center of the contour plots represents the nadir which is $(\theta_r, \phi_r) = (0^\circ, 0^\circ)$ and the distance from the origin is the zenith angle, with forward scattering towards the bottom $(\theta_r, 180^\circ)$ and backscattering towards the top $(\theta_r, 0^\circ)$, respectively. In phase angle plots the

positive phase angles stand for right half plane ($\phi_r \in [0^\circ, 180^\circ]$) and the negative ones stand for left half plane ($\phi_r \in [180^\circ, 360^\circ]$).

The typical REFF of a 10 mm thick dry layer of sample A (0.5 – 1 mm) without an underlying mirror, illuminated by red light, is plotted in Fig. 2, with contour plots in Fig. 2(a) and phase angle plots in Fig. 2(b), respectively. At 0° illumination, the surface is nearly lambertian, with approximately 6% decrease from nadir to 65° viewing zenith. As the incident zenith moves off from nadir, REFF becomes more and more anisotropic with an enhanced backscattering peak showing up near 0° phase angle. Within our available phase angle range, the measured REFF is strongly backscattering. Fig. 3 is the REFF of dry sample A (0.5 – 1 mm) with a 1.2 mm thick layer over the mirror illuminated by red light. The most prominent effect of an embedded mirror below this thin layer is the enhanced reflectance in near-normal incidences 0° and 5° , as seen by comparing Figs. 2 and 3. The specular peak that a mirror would exhibit [3] is not obvious in the REFF at higher incident angles even for such a thin layer. In order to quantify possible thickness-dependent REFF variations for different layers, we have calculated the albedo from the REFF.

The hemispherical reflectance or albedo at each incident zenith angle is defined by:

$$\alpha = \pi^{-1} \int_{2\pi} \int_{\pi/2} REFF(\theta_v, \phi_v) \cos \theta_v \sin \theta_v d\theta_v d\phi_v$$

To evaluate this integral from the available reflectance factor data, the following discrete summations are carried out [5]:

$$\alpha \approx \pi^{-1} \sum_{n=1}^7 \overline{REFF}_n \Delta\Omega_n$$

where $\Delta\Omega_n$ is the projected solid angle:

$$\Delta\Omega_n = \pi(\sin^2 \theta_n - \sin^2 \theta_{n-1})$$

with $\theta_n = 0^\circ, 10^\circ, 20^\circ, 30^\circ, 40^\circ, 50^\circ, 60^\circ, 90^\circ$ for $n=1, 2, \dots, 8$, and

$$\overline{REFF}_n = \sum_{k=1}^m \frac{REFF_n(\theta_n^*, \phi_k)}{m}$$

where θ_n^* are viewing zenith angles satisfying:

$$\theta_{n-1} < \theta_n^* < \theta_{n+1}$$

and ϕ_k are viewing azimuths of the BRDF-meter [3].

We have noticed that when measuring a powdered surface, factors such as the packing density and surface flatness have a large effect on its final albedo values, in contrast to a machined surface which is repeatable with a maximum of 0.3% error. While every measure was taken to ensure grain layers with different thicknesses have the same porosity and flatness, it is impossible to achieve the same precision as a plaque, because of the microscopically random nature of a powdered surface. In Fig. 4 we show two sets of repeated measurements to illustrate the sample-to-sample variability. These samples were a layer depth of 4.5 mm with an underlying mirror, and 10 mm thick layer without a mirror, at red (Fig. 4(a)) and blue wavelengths (Fig. 4(b)). From this experiment we can see the uncertainties caused by preparing the surface are typically less than 1% (Fig. 4(c)). Thus any

albedo variations less than 1% are not attributed to depth variations, but instead to measurement uncertainties.

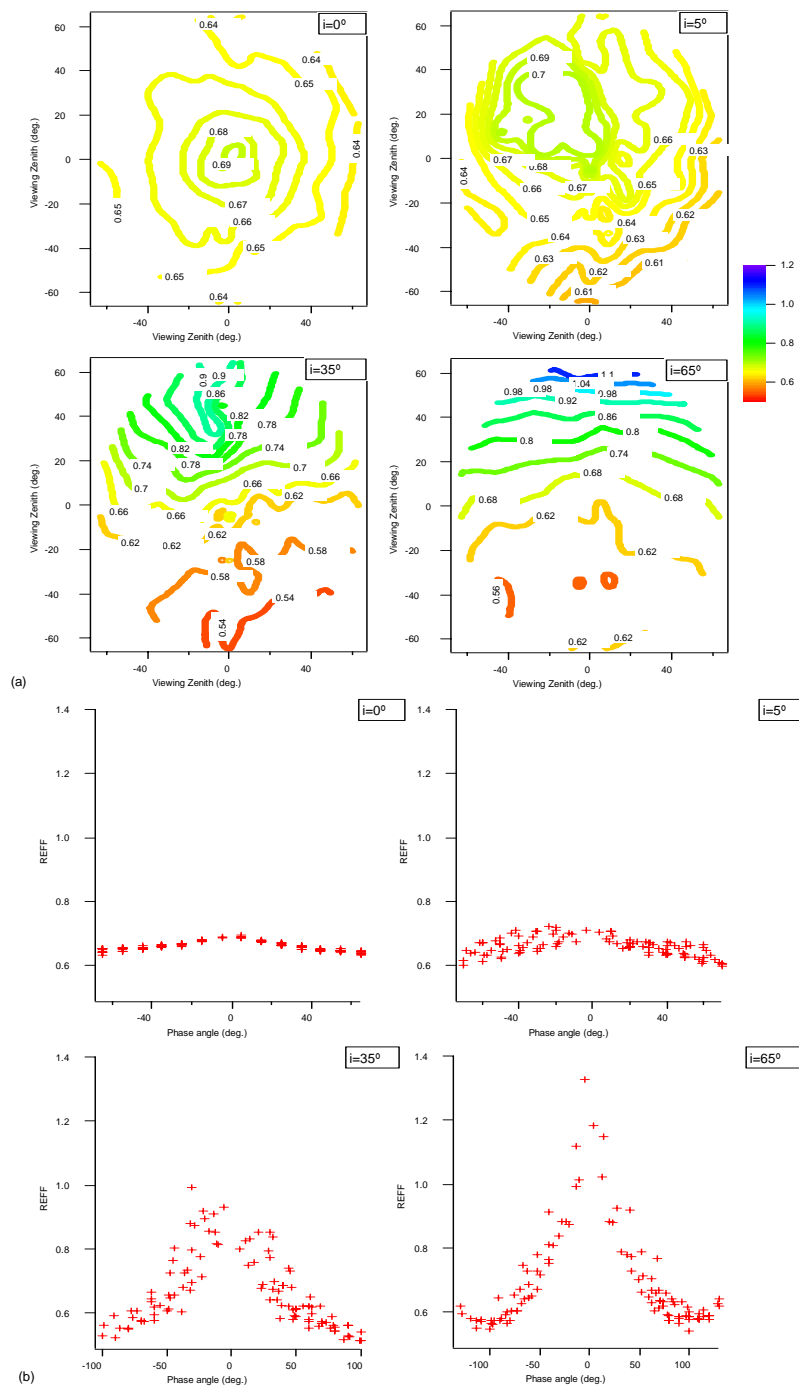


Fig. 2. (a). REFF of a 10mm-thick dry layer of sample A (0.5 – 1 mm) by red light. (b). Same as (a) but REFF is plotted against phase angle. The incident zenith angles are indicated in boxes. See text for viewing angle specifications.

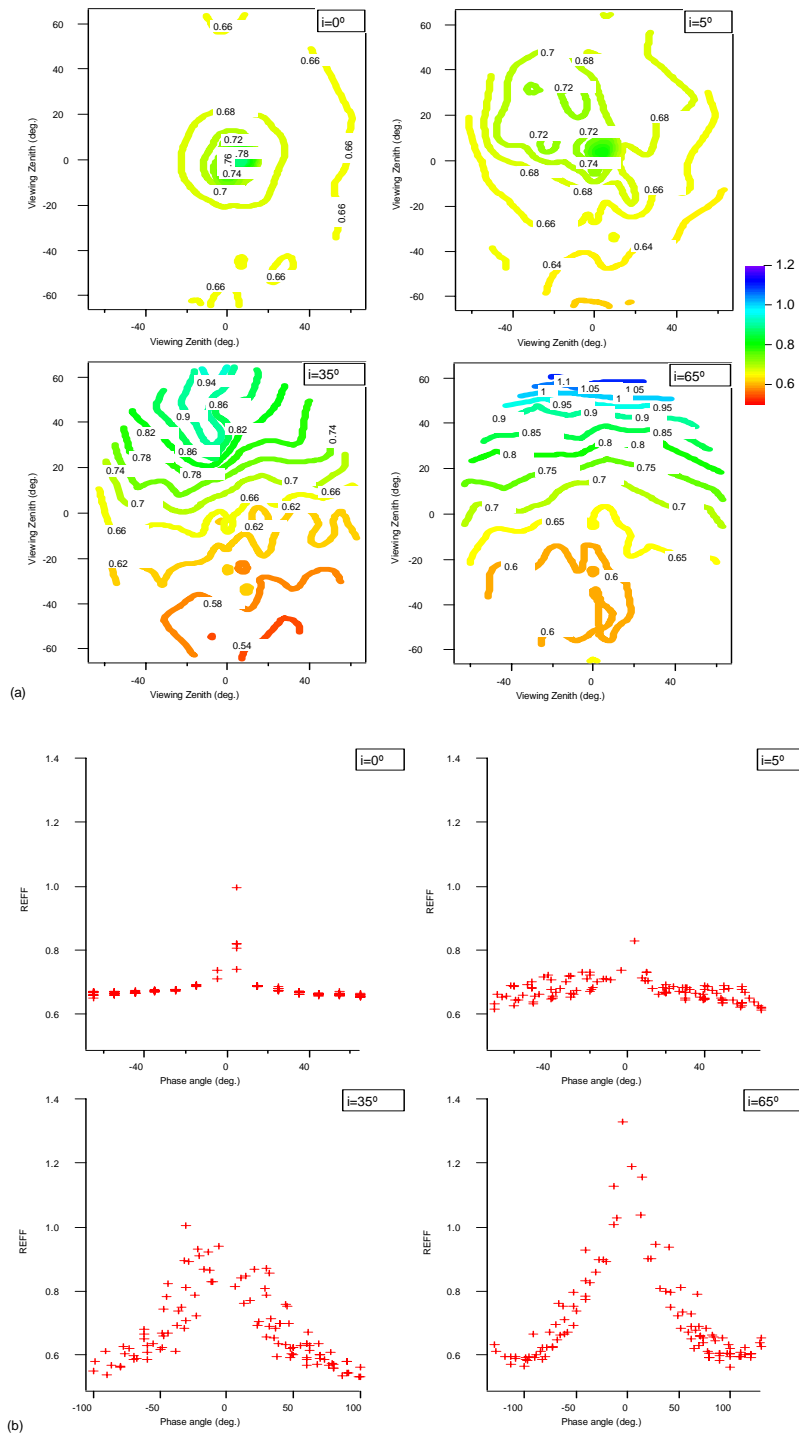


Fig. 3. (a). REFF of 1.2mm-thick dry layer of sample A (0.5 – 1 mm) on mirror. (b) Same as (a) but plotted against phase angle. The incident zenith angles are indicated in boxes. See text for viewing angle specifications.

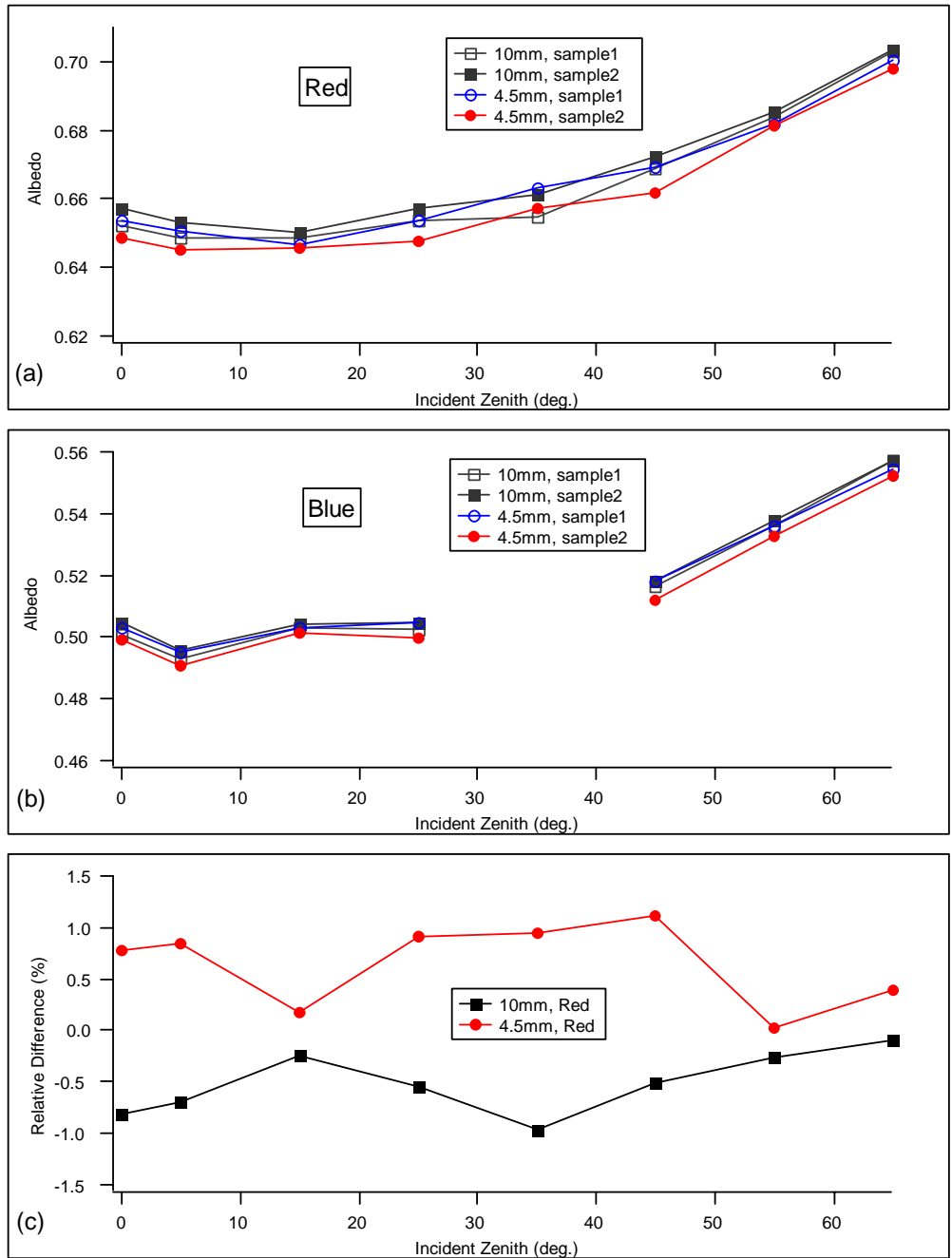
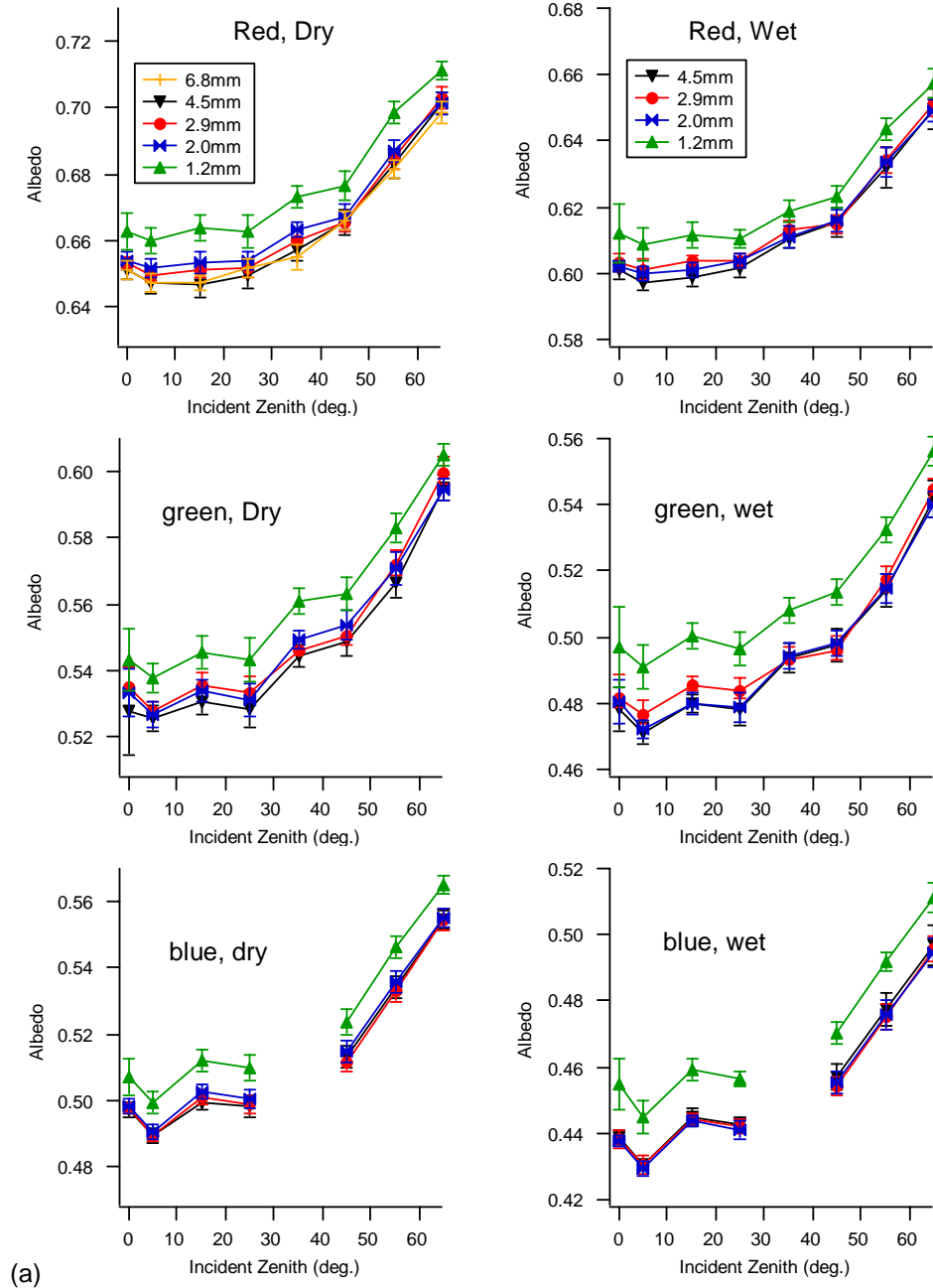
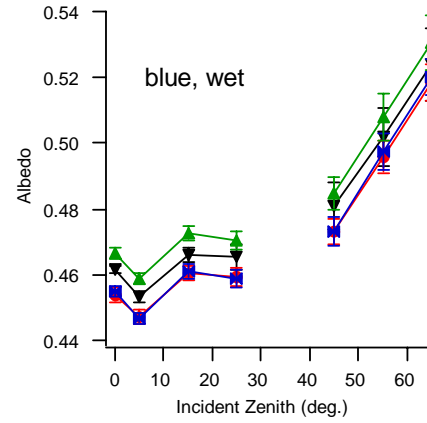
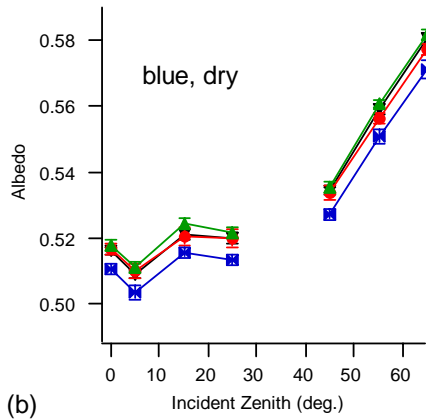
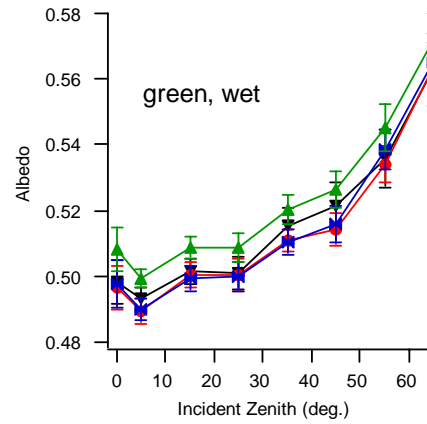
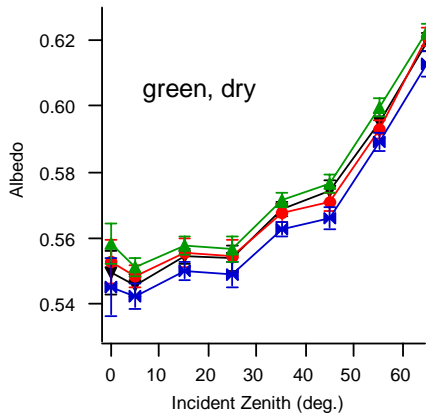
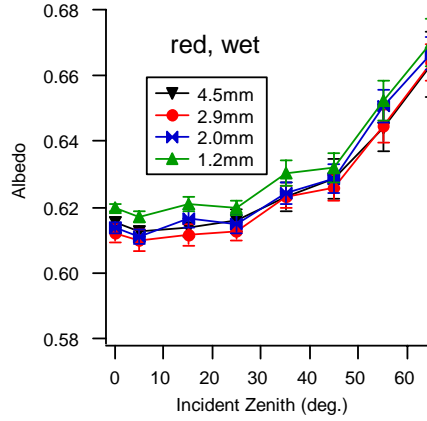
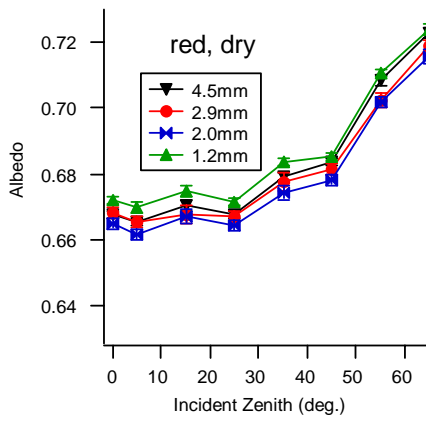


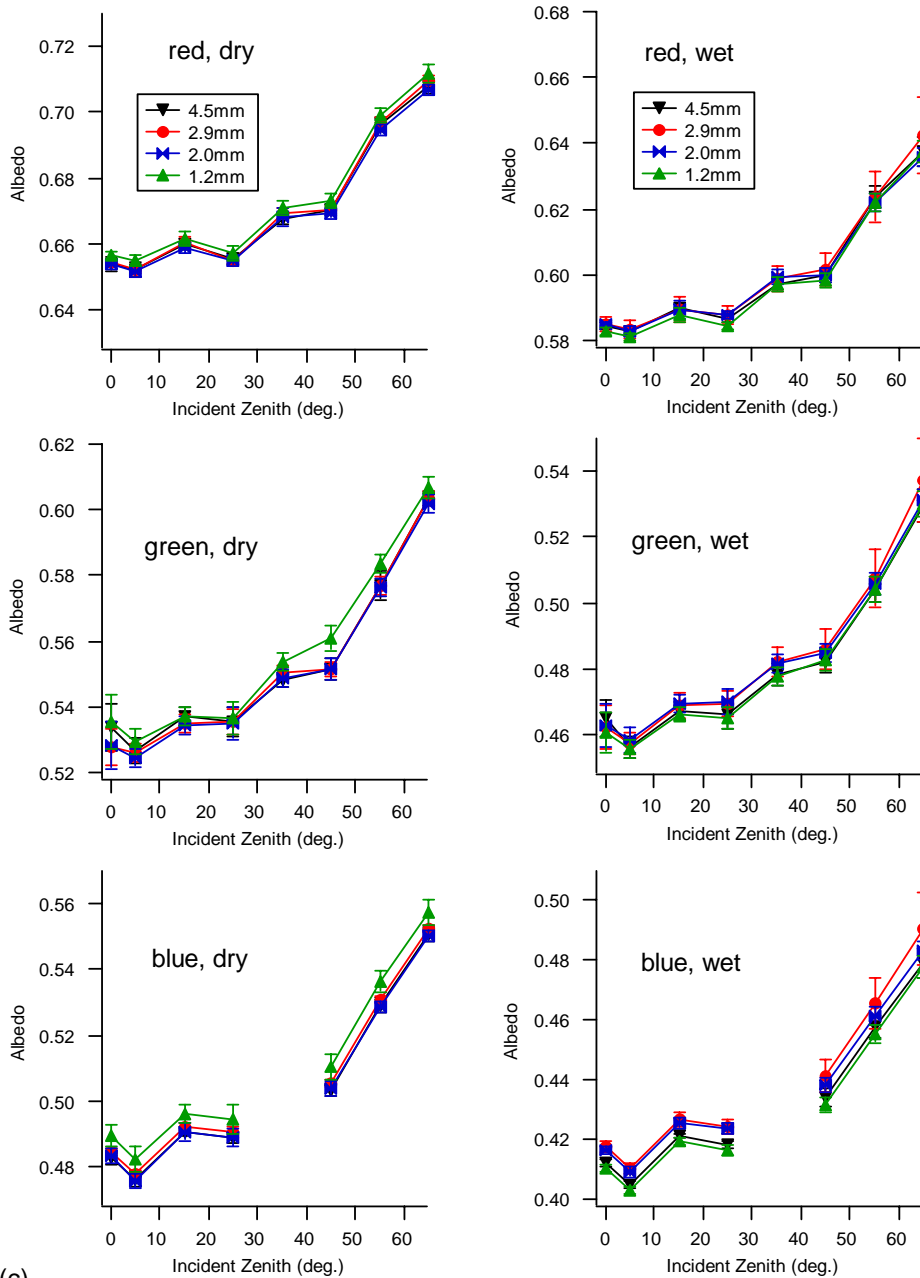
Fig. 4. Repeated measurements on sample A (0.5 – 1 mm) to determine the variability in the albedo for replicate samples probed by (a) red light and (b) blue light. (c) Percent relative differences in the red between two surfaces of 4.5 mm and 10 mm thickness.

The albedo versus incident zenith angles for the three ooid samples at 3 illumination colors are shown in Fig. 5; error bars represent the standard deviation between the sample rotations.





(b)



(c)

Fig. 5. Dry and wet albedos: (a) sample A, 0.5 – 1.0 mm ooids, (b) Sample B, 0.25 – 0.5 mm ooids, and (c) Sample C, 0.125 – 0.25 mm ooids. A broken blue LED caused a void data point at 35-degree incident zenith angle. The 6.8mm layer is very close to 4.5mm layer thus for clarity it is only shown for dry sample A.

For dry sample A, Fig. 5(a) shows that all three wavelengths can see mirror at 1.2mm, but the thicker layers do not show a significant effect. Taking into account measurement uncertainties, a 2 mm layer for the three colors may be regarded as optically thick for sample A. For sample B (Fig. 5(b)) and C (Fig. 5(c)), all colors of light are barely affected by the mirror with layer depths greater than 1.2 mm; as the mirror moves further down, other factors

affecting albedos such as porosity and surface morphology overwhelm the underlying surface. Thus, a 2 mm-thick layer for sample A, B and C can all be regarded as infinitely deep for BRDF and reflectance measurements.

4. Discussion

4.1 Effects of wetting

Overall the wet albedos versus incident zenith are seen to possess the same trends as the corresponding dry ones. All wetted surfaces are substantially darkened since upon wetting the refractive index contrast between grains and the surrounding medium decreases thus forward scattering increases and accordingly more absorption occurs[6]. We plot the REFF of a 1.2 mm thick wet layer of sample A by red light with an underlying mirror in Fig. 6(a) and the relative difference from its dry counter part (shown in Fig. 3(a) $i=65^\circ$ panel), i.e.

$$100 \times \frac{REFF^{wet} - REFF^{dry}}{REFF^{dry}}$$

in Fig. 6(b). One can see the wet REFF increases in the forward direction and backscattering is greatly suppressed, as manifested by the negative values around the hotspot direction (Fig. 6(b)). Even for the thinnest 1.2 mm-thick layer the enhancement of forward scattering induced by wetting is much greater than that the introduction of a mirror, as the comparison of Fig. 2 and Fig. 3 shows.

Since more forward scattering occurs when wetting, one may expect a larger penetration depth in wet layers, as has been observed in measurements with an embedded fiber optic microprobe in quartz sands [7, 8]. Fig. 5 indicates, however, that wetting doesn't cause a larger sensible depth in our BRDF measurements. Although no quantitative control of water concentration was devised for wetting such thin layers, our method should make layers with close to the same water concentration. For sample A, there is very little difference between the effects of layer thickness in wet vs. dry. The albedo of the layer depth 1.2 mm is 1.6% (red) and 3% (green and blue) higher than other thicknesses thus the mirror effect is obvious at this thickness. As the layer thickness increases, the albedo difference between 4.5 mm and 2 mm is within 1%. For wet sample B, layer thickness 1.2 mm is about 1% (red) and 2% (green and blue) higher. For wet sample C however, no significant difference can be detected. This indicates that for wet sample C (0.125 – 0.250 mm), a 1.2 mm-thick layer is indeed infinitely deep in the BRDF measurement.

4.2 Comparison with radiative transfer modeling results

The radiative transfer equation (RTE) [9], though incapable of taking into account factors such as the packing density and surface morphology, may still provide first order estimates of the influential depth by examining the BRDF and albedo for different thicknesses. Liang [10] studied the sensible optical depth in soil by employing the discrete ordinate radiative transfer code (DISORT) [11] for spherical and the T-matrix [12] code for non-spherical particles with varied size distributions. The results show that for large particles, such as sandy soil, the influential depth is about 4 times the effective particle radius. The present BRDF measurements show that for both dry and wet ooids, the discernable penetration depth is at most 2mm. Thus the experimental results agree within the same order of magnitude with radiative transfer calculations. Both results have indicated that geometrical optics might be a better choice over RTE calculations on modeling the sediment reflectance in the optical

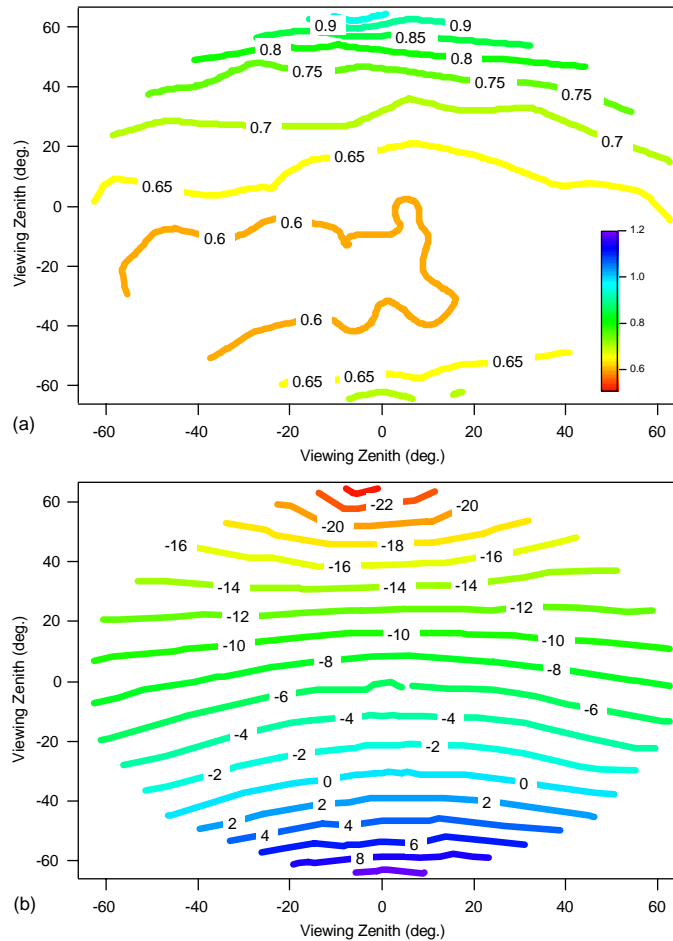


Fig. 6. (a) REFF of a 1.2mm layer of wet sample A at 65-degree incident zenith by red light, see Fig. 3(a) $i=65^\circ$ panel for comparisons. (b) Relative difference of wet and dry REFF of this layer.

region, since the surface roughness and packing structure may be predominant within such a thin layer. Also as mentioned in Section 2, it would be desirable to take into account other environmental factors in order to better extrapolate to actual sediment systems in the ocean. This is the topic of our current work.

Acknowledgments

We thank Albert Chapin for making the sample holder devices and Dr. Eric Louchard for performing the sediment sorting. This work was supported by the Office of Naval Research Ocean Optics Program.